Lifetime Extension of Higher Class UHF RFID Tags using special Power Management Techniques and Energy Harvesting Devices

Alex Janek[1 2], Christian Steger[1], Josef Preishuber-Pfluegl[2] and Markus Pistauer[2]

[1] Institute for Technical Informatics, Graz University of Technology
Inffeldgasse 16/1, 8010 Graz, AUSTRIA
janek,steger@iti.tugraz.at
[2] CISC Semiconductor Design&Consulting GmbH
Lakeside B07, 9020 Klagenfurt, AUSTRIA
j.preishuber-pfluegl,m.pistauer@cisc.at

Abstract. Enhanced RFID tag technology especially in the UHF frequency range provides extended functionality like high operating range and sensing and monitoring capabilities. Such functionality requiring extended system structures including data acquisition units, real time clocks and active transmitters causes a high energy consumption of the tag and requires an on board energy store (battery). As a key parameter of the reliability of an RFID system is the lifetime, the energy budget of the higher class tag has to be as balanced as possible. This can be achieved by using energy harvesting devices as additional power supply. The PowerTag [1] project and thus this paper proposes special power management mechanisms in combination with special energy storage structures interfacing energy harvesting devices and dealing with their special requirements. First various power management and power saving techniques are simulated and their performance is evaluated. In a second step different implementation variants of energy storage structures are compared by using accurate simulation models of the various parts of the system. The results are compared to manufacturer given and guaranteed system performance parameters of a state-of-the-art higher class UHF RFID system. The presented approach combines two simulations for the design and the evaluation of different tag architectures and power saving techniques. Simulation results are showing an improvement of over 44% of achievable lifetime applying the power saving techniques and power subsystem architectures presented in this paper, compared to a state-of-the-art higher class system.

Keywords. Higher Class UHF RFID, Energy harvesting, Energy storage architectures, Lifetime extension

[1] This project has been supported by Austrian government under the grant number 811854

Dagstuhl Seminar Proceedings 07041
Power-aware Computing Systems
http://drops.dagstuhl.de/opus/volltexte/2007/1104

1 Introduction

The next generation of UHF RFID tags (called higher class UHF RFID tags - HCT [1]) provides extended functionality in terms of independent sensing and monitoring, high communication range and large memory areas. This requires continue operation of the tag itself - also if it is not powered by the reader as in formerly pure passive UHF RFID systems [2]. Thus an on-board energy supply is necessary, which forces a renaming of the previously called passive UHF RFID technology to semi-passive and active technology. This change in the tag architecture pushes new issues in the area of UHF RFID; the operational lifetime, which is limited by the on-board energy reservoir and thus the need of long time power saving techniques. The energy, which is stored on a tag is limited by the state-of-the-art energy storage technology and so even with profound power saving techniques the achievable lifetime is often dissatisfying. The way to solve this issue is to supply energy from the environment by energy harvesting devices. As the energy converted by such devices comes from the environment, it is generally unpredictable, non-continues and unstable special energy storage architectures are necessary to deal with this particular requirements, which are presented in the following sections. The difference between semi-passive and active technology is the tag to reader communication. Semi-passive UHF RFID tags provide extended functionality as mentioned before but the communication is based on the same passive method as passive UHF RFID tags simply reflecting and modulating the reader signal. The operating range of such tags is much higher, as the reader signal is used for the communication only but not for powering the whole tag like in pure passive RFID [2]. The communication from tag to reader of active UHF RFID tags is based on an active on-tag communication unit (transmitter), which generates a carrier frequency and modulates it. The difference between the two technologies is the achievable operating range, which is much higher using active UHF RFID technology. This technology additionally is similar to sensor nodes; the difference is that an active RFID system is hierarchically controlled by a central reader whereby the principle of a sensor network is the cooperative (multihob) communication between sensor nodes mostly on the same hierarchical level. The constraints for both active RFID and sensor node systems are similar for many parameters as shown in [3]; cited literature is often based on sensor node technology as more research has been done in this field.

1.1 System structure of higher class UHF RFID Tags

The system structure of a higher class UHF RFID tag consists of several functional blocks as shown at Figure 1. This figure shows the structure of an active UHF RFID tag as an example for a higher class tag. The structure can rawly be divided into three different subsystems: the power and scheduling subsystem, the communication and data processing subsystem and the sensing subsystem.

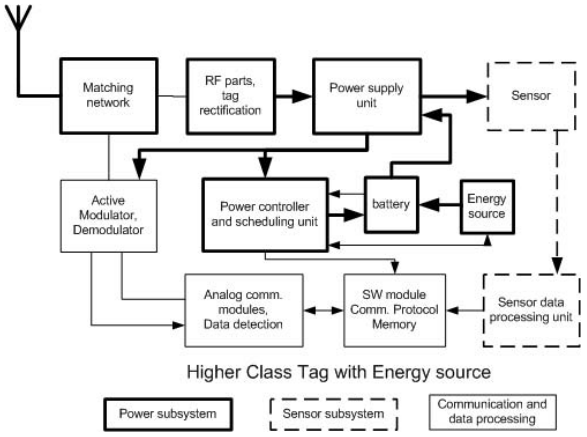

Fig. 1. Higher class tag architecture - Example: active UHF RFID tag

1.2 Energy harvesting

As the mentioned extended functionality of a HCT implies high energy consumption, the key goal for achieving a long lifetime is the optimization of the energy budget of the tag. As this is not possible using single use batteries without replacing them frequently, the target is to use additional energy sources (energy harvesting devices - EHD) to support the on board supply. As the energy converted by energy harvesting devices comes from the environment, it is generally unstable, unpredictable and non-continuous. This requires special power management principles and energy storage structures, which have strong impact on the structure of a higher class tag.

1.3 Related work

The study [4] shows key issues and possible solutions on using solar cells as an energy harvesting device for a sensor node and thus extending the lifetime of the whole system. This study shows that a device including an efficient energy management in combination with a high reliable energy storage and an energy harvesting device is able to operate near-perpetual.

Table 1 is taken from a study [5] and compares energy storage structures and energy harvesting devices in different aspects.

In [6] special energy storage structures are presented, which use environmental radio frequency fields for powering mobile phones. The key goal of the project was to design an energy storage structure being able to convert the scavenged very low power to a level, which can be used to charge the phones batteries. In [7] an energy storage structure including a rechargeable battery interfacing a solar cell as a power supply for a sensor node (Heliomote) is shown and the achieved performance is analyzed. In [8] and [9] several measurements and theoretical considerations are showing, that the energy provided by energy harvesting devices

Power Source	P/cm^3 (μ W/cm^3)	E/cm^3 (J/cm^3)	P/cm^3/Year (μ W/cm^3/Jr)
Primary Bat	-	2280	90
Secondary Bat	-	1080	34
Micro-Fuel Cell	-	3500	110
Ultra-capacitor	-	50-100	1.6-3.2
Heat engine	-	3346	106
Radioactive (Ni63)	0.52	1640	0.52
Solar (outside)	15000	-	-
Solar (inside)	10	-	-
Temperature	40	-	-
Human Power	330	-	-
Air flow	380	-	-
Pressure Variation	17	-	-
Vibrations	200	-	-

Table 1. Comparison of the reliability of energy harvesting devices

is mostly unstable, hart do predict and non-continues. Depending on the environmental energy, which is converted, the variation time period of the provided amount of energy varies between milliseconds and days.

2 Problem analysis: power consumption of higher class tags

As the operation lifetime of higher class tags depends heavily on the energy available in the energy store, a profound and accurate power management managing the power consumption in an intelligent way as well as being able to give a feedback about the expected remaining lifetime is one of the key factors defining the quality of a higher class tag. To define power management policies and find improvable parameters, the analysis of the energy consumption of the most important parts of the tag is necessary.

2.1 Power consumption of a HCT - Example

This section describes such an evaluation of a state-of-the-art active UHF RFID tag to find leading energy consumption factors and blocks. The following table (Table 2) shows a long-run evaluation of the energy consumption of a HCT on the example of an active RFID tag from Identec Solutions [10]. This measurement was done for the time period of a day (24 hours). The temperature logging was activated and set to the interval of 1 minute whereby the related active RFID reader requested the last temperature sample once each hour.

Figure 2 shows the measured power consumption profile for the identification process (450 ms) for a higher class tag (active tag from Identec Solutions [10]). The first channel (CH1) shows the command send by the corresponding active

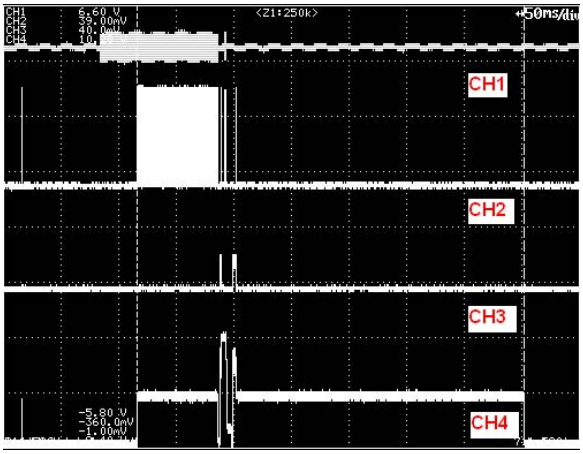

Fig. 2. Communication and current consumption profiles (measured) of an active UHF RFID tag

UHF RFID reader, the second channel (CH2) the digital tag receiver output, the third channel (CH3) the digital response send by the tag and the fourth channel (CH4) the current consumption profile. The action performed is the identification of the tag by the reader and the reading of 16 Bytes out of the tag's memory. The most interesting part is the current profile shown at CH4; easy to see the wake-up current peak of the receiver (periodically each 100 ms) whereby a peak current of *4 mA* is shown (for 0.1 μs - first peak left, CH4) and the identification and memory read part where a peak load of *16 mA* is consumed for 1.2 ms (highest peak - CH4). Additionally, after being woken up, the tag stays in the active mode for around 200 ms, whereby it consumes *5 mA* of current continually.

Standby energy dissipation	0,820 J
Temperature log energy dissipation	0,206 J
Reader interrogation energy dissipation	0,186 J
Memory read (16 byte) energy dissipation	0,109 J
Total energy	1,322 J

Table 2. Energy dissipation

Easy to see at table 2 that the leading factor is the standby current of the system, which includes the current required for periodical readings of the temperature (each 1 minute) and the periodical wake-up of the receiver circuit (each 100ms).

Although the current flow is small, it is consumed continually and so it has a significant impact on the tags lifetime. The proposed solution described in the following sections reduces this current by introducing power saving techniques (e.g. special wake-up procedures) in combination wit the use of energy harvesting devices.

2.2 Energy harvesting devices

Generally speaking a energy harvesting device converts energy from the environment into electrical energy. This fits to the most important and common sources as mechanical energy (vibrations - piezo generator), solar light (solar cells), thermal energy (temperature differences - thermo generator) as well as to less common sources like electromagnetic energy (RF sensor).

Piezo generator The piezo generator is based on the piezoelectric effect whereby piezoelectric materials are deformed on the presence of an electromagnetic field and conversely produce an electromagnetic charge if they are deformed [11].

The following Figure 3 shows the energy generated by a piezo generator produced by smart-material ® [12] equiped with a cantilever system and mounted to a microwave oven (121 Hz vibration [11]).

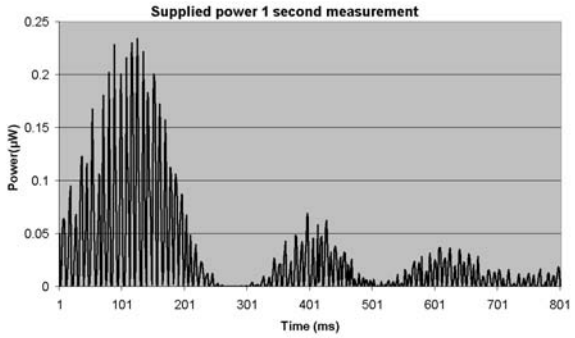

Fig. 3. Measurement of the power supplied by a piezo generator - 1 seconds

Although the power generated seems to be low in this measurement, it depends heavily on frequency and amplitude of the vibrations. A large area of applications of HCT provides enough environmental vibrations to power the entire tag from the claimed energy [11] (e.g. tags on train wagons, big machines...).

Thermogenerator The thermo generator converts thermal energy given through temperature differences between two surfaces based on the so called *seebeck effect [13]* into electrical energy.

Figure 4 shows the energy generated from a thermo generator produced by Thermalforce [14] fixed to a light bulb. The temperature difference between the surface with the head sink and the surface attached to the light bulb was Δ T = 40°C.

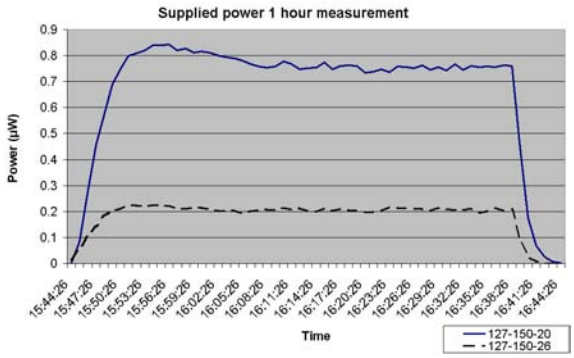

Fig. 4. Measurement of the power supplied by a thermo generator - 1 hour

Although again the claimed power seams to be low, the measurement has been done in a way far from the optimal application and additionally, if it is provided continually it supports the battery significantly.

Solar cells Solar cells are the most common energy harvesting device, accordingly much research and new developments happened recently. The results shown below have been measured using flexible thin film solar cells based on amorphous silicon produced by PowerFilm Solar Inc. (MP4.8-75 [15]).

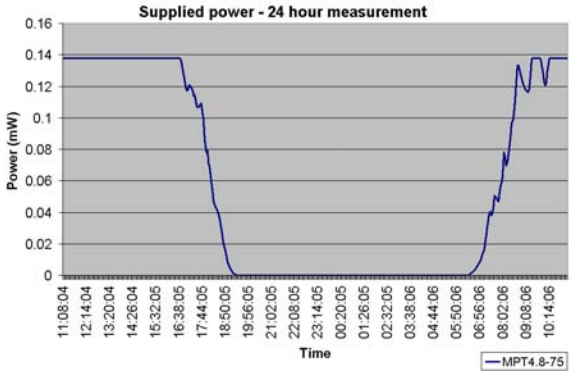

Fig. 5. Full day measurement of power provided by solar cells - sunny day

3 Novel power management strategies for battery-driven higher class tags supported by energy harvesting devices

This section deals with special power saving techniques, which allow to save power on the one side but even to utilize power provided by the reader on the other side.

3.1 Sleep state transition - wake up control

As one of the simplest and most efficient power saving strategies is to keep the system as long as possible in the power saving state (sleep state transition [16]) a very efficient method to save energy is the wake up mechanism. The tag stays in a low power state (sleep or standby) and changes to the active state only triggered by a certain event. This event may be a time tick signal or the output of a low power signal decoder on the reception of a special structured bit pattern. Figure 6 shows the structure of a tag equipped with a special low power wake-up signal decoder.

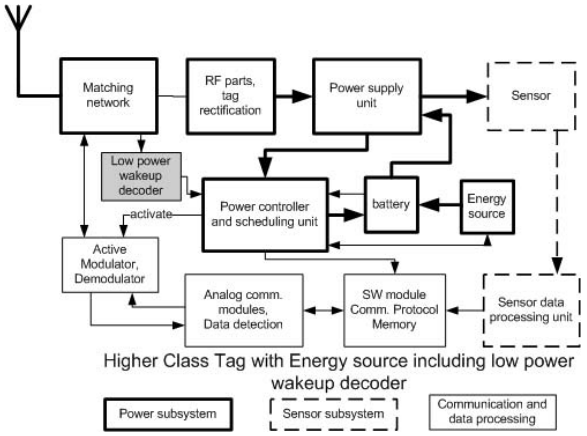

Fig. 6. Structure of HCT including low power wakeup decoder

Upon reception of a special wake up structure sent by the reader the low power decoder activates the main decoding block and the receiving state machine, which processes incoming communication sequences.

3.2 Reader distance measurement

This method is suitable mainly for higher class tags, which are communicating with the reader by passive backscattering and is based on the evaluation of

the distance between tag and reader. This may be done simply measuring the strength of the received reader signal (carrier) or evaluating the distance with complex and accurate distance evaluation mechanisms.

The idea is that depending on the distance between tag and reader, three different operating modes can be defined.

1. The first mode applies if the distance of the tag to the reader is short enough that the tag can be powered by the energy provided by the reader carrier signal. The operation does not require the support of the on board battery, which is switched off. The distance in that case is typically around 5m.
2. The second mode applies if the distance is to high so that the tag can not be powered by the reader signal but the communication with the reader is still possible. The battery is used for powering the tag and its periphery (sensors...). The distance in that case is typically between 8m and 20m.
3. The third mode applies if the distance to the reader is to high so that the signal strength received by the tag is so low that the reader will not be able to receive the reflected signal modulated by the tag. The tag is powered by the battery but it does not respond to received reader commands. The distance in that case is typically higher than 20m.

Figure 7 shows the three mode algorithm. Depending on the distance to the reader the power control unit decides if to enable the battery and if to decode the incoming reader commands.

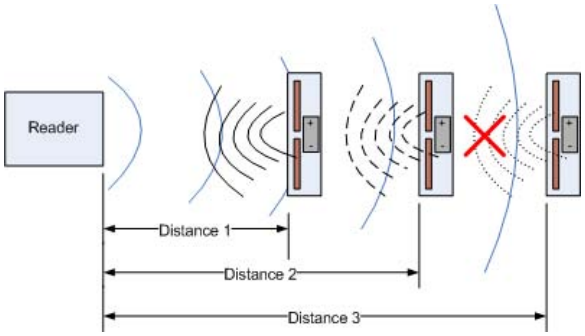

Fig. 7. Three mode algorithm

3.3 Evaluation results

This sections shows results of two simulations (table 3 and table 4; two scenarios describing real world applications for UHF RFID tags have been simulated based on the simulation model mentioned before. Each scenario has been simulated for a tag implementing the power saving algorithm (three mode algorithm - battery only used if necessary) and for a tag with a fixed battery support (always on).

Use case 1 - Container shipment: The first scenario describes the shipment of containers equipped with HCT. During the simulated shipment process of 4 weeks, different readers are trying to inventory the tag on the container 50 times. This happens as an example 10 times by a reader directly near the tag (short distance, < 5m), 20 times in a middle distance (around 20m) and 20 times out of the communication range (long distance, > 20m - the tag is not inventoried). Additionally the tag measures the current temperature each 6 hours and stores the value in its memory. Those values are read out by readers 68 times; 10 times in a short distance, 18 times in a middle distance and 50 times from a long distance (no communication is possible).

Table 3 shows the results of the simulation of scenario 1, the container shipment.

Algorithm	EEPROM	FRAM
Battery always on	1,409Ws	27,5μWs
Reader distance measurement (Three mode algorithm)	1,38Ws	23,0μWs

Table 3. Scenario 1: Container shipment

As visible there is no big difference in the energy supplied by the battery between the simulation of a tag implementing the three mode algorithm and the simulation without this algorithm. The reason is that most of the time the tag is not in a reader field and so the battery has to supply the whole energy for the logging mechanism.

Use case 2 - Public transport access control: The second scenario describes public transport access control and booking. The simulated time is 1 year and it can be assumed that due to mechanical restrictions (gate construction) the tag is always within the range where a communication with the reader is possible. It is assumed that the tag reader communicates 600 times with the tag (nearly 2 times per day) reading and adjusting the account balance. It is assumed that the communication happens 300 times with the tag near the reader (< 5m) and 300 times in the weak field (< 20m).

Table 4 shows the results of the simulation of scenario 2, the public transport access control.

As visible a significant amount of energy supplied by the battery can be saved if the capability of the reader of providing the necessary power to the tag is evaluated. This affects mainly applications where a high percentage of the total communication processes happens in a short distance between tag and reader.

The simulation results have shown that a simple mechanism under certain conditions allows to save around 50% of the power consumed from the tags battery.

Algorithm	EEPROM	FRAM
Battery always on	11,91Ws	0,261mWs
Reader distance measurement (Three mode algorithm)	5,37Ws	0,121mWs

Table 4. Scenario 2: Public transport access control

4 The power subsystem: Energy storage structure

As applying the power saving mechanisms mentioned in the section before (section 3) reduces the power consumed by the tag but this does not improve the lifetime of the tag to the desired level, energy harvesting devices are used as an additional power supply. The special characteristic of energy harvesting devices requires special energy storage and buffer structures, which are the topic of this section.

There are two types of energy storage devices necessary, in order to utilize the energy provided by energy harvesting devices in an efficient way and to be able to guarantee a certain minimum lifetime: a primary and a secondary energy storage. The primary energy storage is not rechargeable, but guarantees a certain energy and thus lifetime, whereby the secondary energy storage is able to be charged/discharged several times depending on the amount of energy provided by the energy harvesting device.

4.1 Primary energy storage

The primary (single use) energy storage guarantees a certain minimum lifetime even if no energy is provided by the harvesting device. Nowadays higher class UHF RFID systems are mostly based on primary batteries; thus the lifetime is limited but guaranteed for a certain period of time under particular conditions. After this period the battery has to be replaced - if possible - otherwise the full tag must be changed. As an example, the manufacturer of higher class RFID systems, Identec Solutions [10], guarantees for a higher class active UHF RFID tag equipped with a primary battery with 2.2 Ah of capacity under certain conditions (600 memory readings/day) a operational lifetime of 4 to 6 years.

There exist several different types of primary energy storage devices; the most important ones are described in the following section.

Nuclear battery: The most common types of nuclear batteries are betavoltaic batteries and batteries based on the piezogenerator principle [8]. The betavoltaic battery works similar to a solar cell. The only difference is that instead of the sun as a source for radiation, a radioactive material is used. The radioactive piezogenerator is based on a piezoelectric material fixed to a cantilever beam that is excited through particles from a radioactive material.

Type	Betavoltaic battery	Nuclear piezogenerator
Material	Ni-63	Ni-63
Half life	100 years	100 years
Power	150 nW @ 100 mCurie	15 μW @ 0.5 mCurie

Table 5. Battery capacity, material and lifetime of nuclear batteries

Electrochemical cells: The most common primary (non-rechargeable) electrochemical battery types used in portable electric devices and consumer electronics are: Zinc-Carbon, Alkaline-Manganese Dioxide and Lithium. The working principle is similar to all types, the difference is the energy density, voltage per cell and the sensitivity against environmental impacts [17].

Microcells: Microcells or microbatteries are based on the same working principle as standard-size electrochemical cells. However, the used materials are different. Due to the reduced size the capacity is significantly reduced, limiting their applicability to very low power applications.

4.2 Secondary energy storage

The secondary (rechargeable) energy storage fulfills two main tasks. It deals with the special requirements of energy harvesting devices being charged on a surplus of environmental energy and being discharged on lack of environmental energy. Additionally, it buffers current peaks generated by the higher class tag. Two main types of secondary energy stores are described in the following section.

Electrochemical capacitors: Electrochemical capacitors are capacitors with high energy density. These properties come from an electrochemical double-layer and the use of high conductivity materials as well as from the large surface area of the electrodes, which is achieved by using porous materials [18]. Differences between an ultracapacitor and a rechargeable battery are the nearly unlimited cycle life and the fact, that ultracapacitors have nearly no negative battery effects apart from a high self discharge rate [18,19,20].

Electrochemical cells/microbatteries: The working principle of rechargeable (secondary) electrochemical cells is similar to the single use (primary) types as described in section 4.1 and 4.1 but the materials are different.

5 Novel power subsystem architectures for higher class tags

The following sections show two possible implementation variants of the energy storage architecture, which will be compared in the simulation subsequently. Table 6 and table 7 are pointing out different advantages/disadvantages of the implementation variants. Variant 0 describes the higher class tag directly connected

to a primary battery and is used in the simulation as reference implementation to show related improvements.

5.1 Variant 1 with two ultracapacitors as secondary energy storage

Figure 8 shows the first implementation variant, which includes two ultracapacitors, being charged by the energy harvesting device. The ultracapacitor, which is not charged at the moment provides the power for the operation of the higher class tag. The other ultracapacitor is charged in the meantime (by the energy harvesting device) and vice versa. This allows an efficient charging and discharging of the capacitors and to keep the ultracapacitors in the optimum charge state (with the lowest self discharge rate). If the power supplied by the energy harvesting device is low and the power consumed by the HCT is high at the same time, it may happen that both ultracapacitors are on low charge state. In that situation the primary battery directly supplies the HCT (P_S).

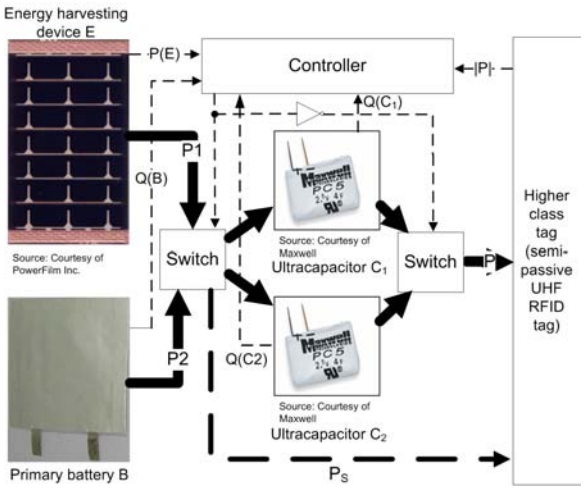

Fig. 8. Energy storage architecture variant 1 with two ultracapacitors

5.2 Variant 2 with two ultracapacitors as secondary battery and additional third (smaller) capacitor

The second implementation variant is nearly the same as the first one (section 5.1). The differences are an additional smaller capacitor, which provides the power while both ultracapacitors are charged and the extension that the two ultracapacitors are charged by the battery to, when the power supplied by the energy harvesting device is too low to operate the tag. So the battery is completely decoupled from the HCT, which is important as peak current loads are

Advantages	Disadvantages
Efficient (one capacitor charged while the other is discharged)	Complex controller application
Ultracapacitors operated in best work point (low self discharge)	Doubled self discharge current compared to variant 1
	Battery directly connected to HCT if both ultracapacitors are charged (current peaks)

Table 6. Advantages/disadvantages of variant 1 with two ultracapacitors

affecting the state of charge of the battery significantly. Those peaks are buffered by the ultracapacitor by this implementation variant.

Advantages	Disadvantages
Highly efficient	Complex controller application
Battery never connected directly to HCT	Expensive (two ultracaps, controller and buffer capacitor needed)

Table 7. Advantages/disadvantages of variant 2 with two ultracapacitors and a small buffer capacitor

6 Simulation model for the verification of energy storage architectures

6.1 Model structure

The simulation model is implemented based on Matlab Simulink® and includes 5 main blocks: battery model, the model of the ultracapacitor, discharge current profile lookup table, the energy harvesting device power supply lookup table and the charge/discharge controller. Each of those blocks is implemented as a behavioral model of the block in the real implementation. Figure 9 shows the overview of the model structure.

In the following subsections each main block is described in detail.

6.2 Stochastic battery model

The battery model block includes the model of the battery based on the stochastic model approach [21]. The capacity of the battery is modeled as a discrete

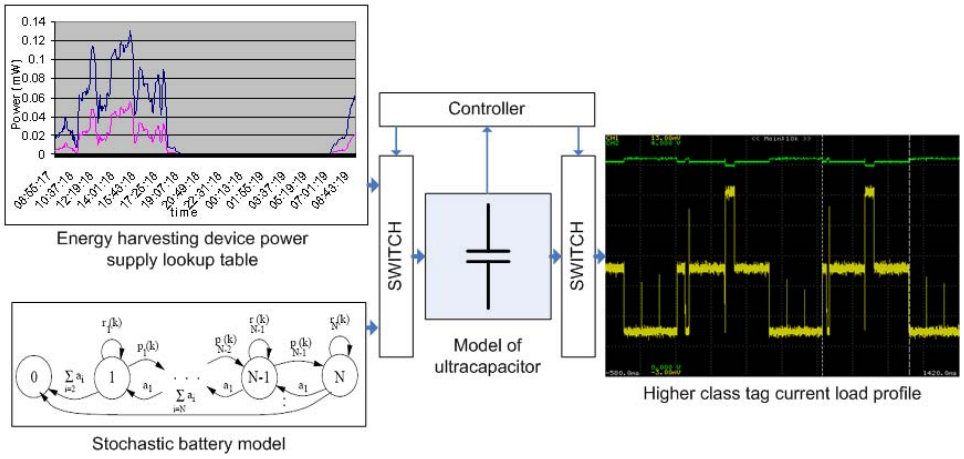

Fig. 9. Basic blocks of the simulation model

time transient stochastic process including the charge recovery as a decreasing exponential function of the state of charge and discharged capacity. The main parts of the battery model are:

- A random number generator needed for the recovery probability.
- A lookup table which interpolates the available capacity at a given rate of discharge.
- The probability function, generating the likelihood of a recovery event.
- A state machine, which keeps track of the states and their transitions.

Based on the original model [21] some modifications were necessary as some battery effects were missing in the original model and others were modeled under theoretical assumptions, which did not comply to real measured systems.

6.3 Model of the ultracapacitor/switch

The model of the ultracapacitor is based on the accumulation of the current; it includes the leading disadvantage of ultracapacitors: the high self discharge. The implementation of the model is based on considerations from [22] and [18]. The switch controls the connection of the ultracapacitors with the discharge profile and with the power supply.

6.4 Higher class tag current load profile lookup table

This model block implements the measured current profile as described in section 2.1. It is implemented as lookup table containing the measured values. This allows to measure the current profile for each desired action performed by the higher class tag and to reuse the measured profile as required.

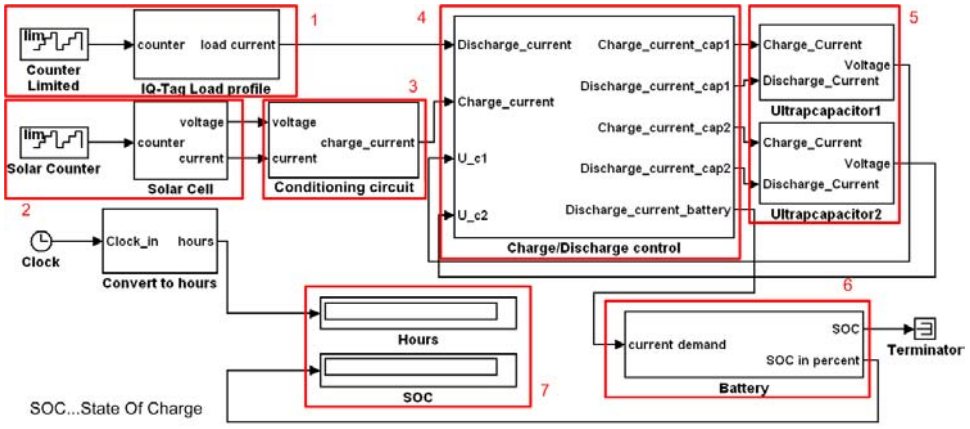

Fig. 10. Detailed structure of the simulation model

6.5 Energy harvesting device power supply lookup table (e.g. solar cell)

Based on the measurements mentioned in [8] a lookup table containing the power values supplied by the energy harvesting device (in the example shown as a solar cell) is created, which defines the power value supplied depending on the simulated timestamp.

6.6 Charge/Discharge controller

The charge/discharge controller controls the charging of the ultracapacitors. Depending on their charge state and on the amount of energy supplied by the energy harvesting device it controls the charging process. On the other hand it decides which of the ultracapacitors is charged and which one supplies power to the tag.

7 Results

This section describes simulations and related results with the goal of the verification of the simulation model (mainly the battery model) by comparing simulation results with parameters from battery data sheets. Additionally, the implementation variants 1 and 2 (section 5) are compared under various aspects by simulating the complete system including energy harvesting device and the current load profile of the higher class tag. This allows to choose the best implementation method for the energy storage architecture.

Figure 10 demonstrates a screenshot of the MATLAB/Simulink® implementation of the model. The figure shows a more detailed view of the simulation model. The function of the blocks is as follows:

1. *Current load profile lookup table:* This block contains the measured current load profile, which is used as load current in the model.
2. *Solar cell:* This block contains the power supply lookup table; a solar cell as example energy harvesting device has been measured for 24h.
3. *Conditioning circuit:* This is a simple implementation of a DC/DC converter.
4. *Capacitor charge control:* This block is the implementation of the controller. It monitors the charge state of the single ultracapacitor and charges it by using the battery or the solar cell.
5. *Ultracapacitor:* This block contains a simple model of the ultracapacitor.
6. *Battery:*This block contains the modified stochastic model of the battery as mentioned in section 6.2.
7. These two displays are showing the simulation results: the simulated number of hours and the corresponding charge state of the battery.

7.1 Verification of the battery model

The verification of the correctness of the implementation of the battery model has been done comparing two simulation scenarios with two measurement scenarios, which are mentioned in the datasheet of the simulated battery (Sonnenschein Lithium SL760 battery [23]). The first scenario is the pulse discharge behavior with a predefined pulse discharge profile and the second scenario the constant current discharge scenario. Table 8 compares simulation results with related datasheet values. The pulse discharge profile is composed of periodical current pulses of 140 mA with a duration of 10 s, 6 times per hour. This is the worst case assumption whereby the battery lifetime has been simulated and measured. For the constant current discharge profile the discharge current has been set to 60 μA.

Discharge profile	**Simulated operating time**	**data sheet value**	**Error**
140 mA peak pulse profile	663 h	690 h	3.9 %
60 μA constant current	30.833 h	30.833 h	0 %

Table 8. Simulation results - verification

As shown at table 8 comparing the simulated operating time with the datasheet values, the accuracy of the simulation is very high.

7.2 Comparison of variant 1 and variant 2

This simulation has been done with the model including the full target system; the energy harvesting device power supply lookup table (power profile of a solar

cell for 24h) together with the model of the battery and the current load profile of the higher class (active) tag. The current load profile used for the simulation has been chosen to comply with the scenario in the data sheet describing the higher class tag used for the current load profile measurement (section 2.1) - 600 readings of 16 memory bytes per day. Table 9 compares results of the simulation of all three implementation variants including all simulated parts with the simulated operating time of the original system (with just the primary battery).

Implementation variant	**Discharge profile**	**Simulated operating time**	**Improvement compared to variant 0**
Variant 0 (original system section 5)	600*16 bytes/day	35.040 h (4 years)	-
Variant 1 (section 5.1)	600*16 bytes/day	41.650 h (4.7 years)	15,6 %
Variant 2 (section 5.2)	600*16 bytes/day	63.000 h (7.1 years)	44,3 %

Table 9. Simulation results - Comparison, full system

As demonstrated at table 9 a significant increase of the operational lifetime was achieved by the implementation variant 1 compared to the original implementation (variant 0). As the absolute amount of power provided by the energy harvesting device is low (around 3 V, 15 μA), the ultracapacitors are just slowly charged and so it is required frequently, that the battery has to directly provide the power to the HCT. As current peaks are reducing significantly the charge of the battery this reduces the benefit of using two capacitors in variant 1. Variant 2 decouples the battery completely from the tag and uses the battery to charge the ultracapacitors; a significant improvement in the lifetime is achieved as the current peaks are buffered all the time by the ultracapacitors.

8 Conclusion

This paper has shown that by using special power saving mechanisms, a significant amount of power can be saved on the operation of higher class tags. Additionally it is shown that the achieved lifetime was significantly improved by using energy harvesting devices in combination with different implementation variants of the tag's power subsystem. The combination of both approaches allows to reduce the capacity of the on-board energy storage significantly and to save size and weight or to improve computational capabilities of the tag achieving the same lifetime. As shown in this paper, the verification method (based on simulation and modeling) facilitates a pretesting of various energy storage architectures to find best suitable implementation for a certain area of applications and in parallel to accurately estimate the achievable lifetime of the tag. On

the other hand it allows to test the performance of various application specific power saving mechanisms. The approach presented in this paper combines two simulations to design and evaluate different tag architectures and power saving techniques. Simulation results have shown an improvement of 44% of achievable operational time compared to a state-of-the-art higher class system aplying the power saving techniques and power subsystem architectures presented in this paper.

References

1. EPCglobal Inc : EPC Radio-Frequency Identity Protocols Class-1 Generation-2 UHF RFID Protocol for Communications at 860 MHz 960 MHz Version 1.1.0. (2007) 8–9
2. Finkenzeller, K.: RFID handbook: fundamentals and applications in contactless smart cards and identification. Second edn. John Wiley and Sons, New York, NY, USA; London, UK; Sydney,Australia (2003) http://www.loc.gov/catdir/toc/wiley031/2002192439.html.
3. Bilstrup, U., Wiberg, P.: An architecture comparison between a wireless sensor network and an active rfid system. Halmstad University (2005)
4. Raghunathan, V., Kansal, A., Hsu, J., Friedman, J., Srivastava, M.: Design Considerations for Solar Energy Harvesting Wireless Embedded Systems. In: Information Processing in Sensor Networks, 2005. IPSN 2005. (2005) 457 – 462
5. Roundy, S., Steingart, D., Frechette, L., Wright, P., Rabaey, J.: Power sources for wireless sensor networks. Australian National University, Engineering Department, AUSTRALIA (2004)
6. Harrist, D.: Wireless Battery Charging System using Radio Frequency Energy Harvesting. University of Pittsburgh, 2001 (2001)
7. Raghunathan, V., Kansal, A., Hsu, J., Friedman, J., Srivastava, M.: Design Considerations for Solar Energy Harvesting Wireless Embedded Systems. In: University of California, Los Angeles, CA 90095. (2005)
8. Janek, A., Steger, C., Preishuber-Pfluegl, J., Pistauer, M.: Power Management Strategies for Battery-driven Higher Class UHF RFID Tags Supported by Energy Harvesting Devices. In: AUTOID2007, IEEE Workshop on Automatic Identification Advanced Technologies, Alghero, Italy. (2007)
9. Paradiso, J., Starner, T.: Energy scavenging for mobile and wireless electronics. In: IEEE Pervasive Computing. (2005) 18–27
10. Identec Solutions GmbH: (Active UHF RFID system) http://www.identecsolutions.com.
11. Roundy, S.: Energy scavenging for wireless sensor nodes with a focus on vibration to electricity conversion. B.S.(Brigham Young University) 1996, M.S. (University of California, Berkerley) 2001 (2001)
12. Smart Material GmbH: (Advanced Piezo Composites) http://www.smart-material.com.
13. Pollok, D.D.: Thermoelectricity - Theory, Thermometry, Tool. ASTM International (1985)
14. thermalforce.de: (Thermogenerators) http://thermalforce.de.
15. PowerFilm Solar Inc.: (Thin flexible solar panels) http://www.powerfilmsolar.com/.

16. Sinha, A., Chandrakasan, A.: Dynamic power management in wireless sensor networks. Massachusetts Institute of Technology, IEEE Design & Test of Computers 2001 (2001)
17. Linden, D., Reddy, T.B.: Handbook of batteries. Third edn. McGraw-Hill edition (2002)
18. Bullard, G.L., Sierra-Alcazar, H., Lee, H.L., Morris, J.L.: Operating principles of the ultracapacitor. In: IEEE Transactions on magnetics, vol 25. (1989) 102–106
19. Zheng, C.: High pulse power system through engineering battery-capacitor combination. In: IECEC International Energy Conversion Engineering Conference and Exhibit, 2000. (2000)
20. Koetz, R., Carlen, M.: Principles and Applications of Electrochemical Capacitors. In: Electrochimica Acta 45,2000. (2000) 24832498
21. Panigrahi, D., Chiasserini, C., Dey, S., Rao, R., Raghunathan, A., Lahiri, K.: Battery life estimation of mobile embedded systems. In: VLSI Design, 2001. Fourteenth International Conference on. (2001) 57–63
22. Joeri, V.M., V.d.Bossche, P., Maggetto, G.: Models of energy sources for EV and HEV: fuel cells, batteries, ultracapacitors, flywheels and engine-generators. In: Journal of Power Sources 128. (2004) 76 – 89
23. Sonnenschein Lithium GmbH: (Sonnenschein lithium batteries) http://www.sonnenschein-lithium.de/.